Improving Masked Autoencoders by Learning Where to Mask

Haijian Chen* Wendong Zhang* Yunbo Wang† Xiaokang Yang† MoE Key Lab of Artificial Intelligence, AI Institute, Shanghai Jiao Tong University

{higerchen, diergent, yunbow, xkyang}@sjtu.edu.cn

Abstract

Masked image modeling is a promising self-supervised learning method for visual data. It is typically built upon image patches with random masks, which largely ignores the variation of information density between them. The question is: Is there a better masking strategy than random sampling and how can we learn it? We empirically study this problem and initially find that introducing objectcentric priors in mask sampling can significantly improve the learned representations. Inspired by this observation, we present AutoMAE, a fully differentiable framework that uses Gumbel-Softmax to interlink an adversarially-trained mask generator and a mask-guided image modeling process. In this way, our approach can adaptively find patches with higher information density for different images, and further strike a balance between the information gain obtained from image reconstruction and its practical training difficulty. In our experiments, AutoMAE is shown to provide effective pretraining models on standard self-supervised benchmarks and downstream tasks.

1. Introduction

Inspired by the masked language modeling framework, masked autoencoder (MAE) [16, 42, 23], also known as masked image modeling (MIM), has been introduced to computer vision and become a promising self-supervised learning method based on Vision Transformer (ViT) [12]. The general idea of this framework is to extract semantic representations by learning to maximize the log-likelihood function of the unobserved patches of input images.

There are two problems that are coupled and crucial to the quality of the learned representations: First, how to determine the masks over the images? Second, how to learn from the masked images? Previous literature has not been able to analyze the first problem sufficiently and satisfactorily in spite of its importance to the learning results. Further, the solutions to "where to mask" and "how to learn from the masked data" have never been integrated into an end-to-end optimization scheme.

What should be a good masking strategy? In general, the difficulty of pixel reconstruction is related to the information density of corresponding image patches. It is a paradox that if we mask a large number of "hard" patches (such as foreground objects), the model may fail to perceive the high-semantic areas; However, if we mask a large number of "easy" patches (such as the background), the self-supervised training task can be too simple for the model to learn effective representations. In our preliminary experiments, we find that both scenarios result in the degeneration of the learned visual representations, as illustrated in Section 2. We refer to such an empirical phenomenon as the patch selection dilemma in MAE.

Therefore, we need to weigh between the informative and less-informative patches in the masking strategy, such that during pixel reconstruction, the model can be trained to reason about the relations between the missing semantics and the remainders. The random masking approach in the original MAE [16] cannot adaptively perceive the variation of information density and applies a unified masking probability over the entire image. Following this line, SemMAE [23] presents a two-stage MAE training scheme with a manually designed *easy-to-hard* masking scheduler, guided by an independently trained semantic part indicator. However, the existing approaches do not directly optimize the masking strategy, thus leading to sub-optimal solutions to constructing the pretext task.

In this paper, we propose AutoMAE, a pilot study of optimizing the masking strategy in a fully differentiable MAE framework. As shown in Figure 1, we compare the key differences between AutoMAE and previous work. The key insights are two-folded: First, it exploits an adversarially trained mask generator, in which the output masking probabilities are correlated with sample-specific information density across the patches, and are prone to be higher for "hard-to-reconstruct" regions in the foreground. Second, it jointly optimizes the mask generator and the self-supervised ViT model through Gumbel-Softmax reparameterization. Intu-

^{*} Equal contribution.

[†] Corresponding authors.

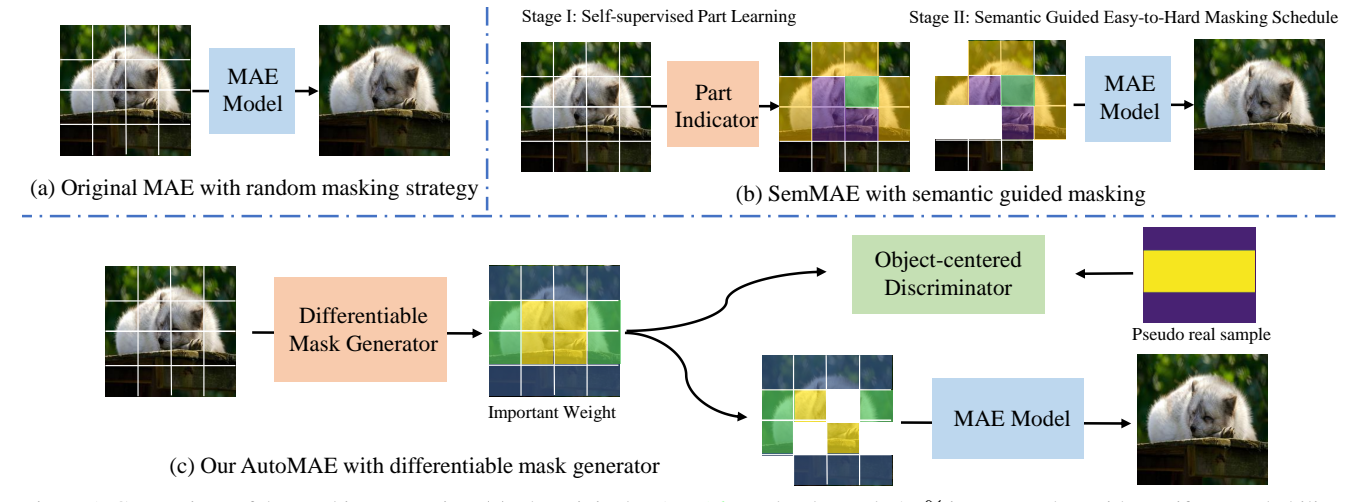


Figure 1. Comparison of the masking strategies. (a) The original MAE [16] randomly masks 70% image patches with a uniform probability. (b) SemMAE [23] uses a manually designed *easy-to-hard* masking schedule guided by an independently-trained semantic part indicator. (c) AutoMAE is a fully differentiable framework that integrates an adversarially-trained mask generator into masked image modeling.

itively, we may prevent the mask generator from overfitting the "hard" regions by back-propagating the reconstruction error of the unobserved patches through the entire model.

Our approach achieves competitive results in the linear probing and finetuning setups on ImageNet-1K [10]. Furthermore, it presents excellent transfer learning ability on CUB-Bird [37], Stanford-Cars [22], iNaturalist 2019 [36], COCO [26], and ADE20K [47] for fine-grained classification, detection, and segmentation, especially on small datasets with limited finetuning data.

The main contributions of this paper are as follows:

- We explore the masking strategies in MIM and demonstrate that the previous random sampling method is suboptimal. We find that the pretraining results can be significantly improved by slightly raising the masking rates of the informative foreground image patches.
- Motivated by these findings, we provide an early study of adversarial mask generation, which incorporates simple structural priors into the adaptive masking rates.
- Unlike prior work, we propose to *integrate mask generation and image reconstruction in a differentiable framework with Gumbel-Softmax*. It improves the pretraining results by striking a balance between the information gain through image reconstruction and its training difficulty.

2. Preliminaries

In this section, we first review the MAE framework and then present preliminary results that learning to reconstruct more informative foreground image patches can significantly improve the learned visual representations. These observations inspire the design of AutoMAE.

2.1. Rethink the Mask Sampling Strategy in MAE

Revisiting MAE [16]. The learning process of MAE can be formalized as the following three steps. First, given an image $I \in \mathbb{R}^{c \times h \times w}$ where h, w and c represent the image height, width, and channel numbers, respectively, MAE first divides the input image into $n = hw/p^2$ non-overlapping patches with spatial size equal to $p \times p$, where p is the patch size. Then these divided patches are embedded by a linear projection layer and added with position embeddings to get the embedded tokens $oldsymbol{Z} = \{oldsymbol{z}_i\}_{i=1}^n, oldsymbol{z}_i \in \mathbb{R}^d$ where d represents the token dimension. Next, in the encoding stage, MAE randomly selects only 25% image tokens combined with a learnable [CLS] token $z^c \in \mathbb{R}^d$ to form the input for the transformer-based encoder. These tokens are served as visible hints and processed by the encoder to obtain encoded tokens Z_e . Given these embedded tokens, MAE starts the masked image modeling process which includes two stages: the encoding stage for visible token interactions and the decoding stage for removed content reconstruction. Finally, in the decoding stage, a shared mask token $z^m \in \mathbb{R}^d$ is repeated and used to fill the places of previously dropped tokens. These repeated mask tokens combined with encoded tokens Z_e are further processed by the transformer-based decoder to reconstruct the pixel values for each dropped patch. The model is optimized by minimizing the reconstruction loss \mathcal{L}_{recon} in dropped regions.

Patch masking strategies. Among the above three steps, the masking strategy plays an important role in masked image modeling, which determines what kind of information will be learned. Although MAE adopts a high masking ratio, image patches are still dropped with equal probability. This random masking strategy ignores the difference in the information density between different patches and results in

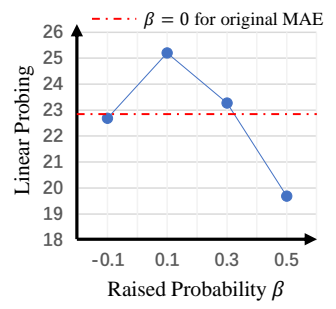




Figure 2. Effects of raising the masking probability by β on patches within the object bounding boxes. Models are trained on a subset (10%) of the ImageNet dataset. The red dashed line rep-

an ineffective learning process.

Two-stage MAE. To improve the random masking strategy, SemMAE [23] exploits a two-stage framework that first learns the possible semantic parts without supervision and then uses the learned partition to determine which token should be masked. The high-quality part-level partition learned by SemMAE can be seen as local semantic guidance to help learn more informative image patches. However, SemMAE still needs a manually designed easy-tohard masking schedule to regularize the learning process and the semantic number is fixed among different images.

resents the results of using the original random masking strategy.

2.2. Key Findings: MAE with Prior Object Hints

Unlike language modeling, the information density of images is more sparse and usually dominated by the objects that appear in the image. Therefore we conduct a preliminary experiment to explore whether introducing the object location priors with high information density can help representation learning. We randomly select a subset (10%) of the ImageNet dataset [10] and use the provided true object bounding boxes to indicate object locations. Instead of random masking, we manually raise the dropped probability of patches within the bounding box and use these samples for self-supervised pretraining. We experiment with different values and show the linear probing results in Figure 2, where β represents the additionally raised probability for patches within the bounding box against those in the background. We have two observations from Figure 2:

- Compared with random masking, slightly increasing the masking probability for patches within the bounding box significantly improves the linear probing results.
- Excessively raising the masking probability of patches within the bounding box may affect the validity of the pretext task and degrades the performance.

These results indicate that different image patches provide different effects on the learning of visual representations, and learning to reconstruct more foreground objects with higher information density can lead to better pretraining results. Nonetheless, we need to strike a balance between the information gain through masked image modeling and its training difficulty. Inspired by this, a natural solution is to integrate mask generation and image reconstruction into a fully differentiable framework. For different images, it can adaptively provide masking weights that reflect prior object hints and are friendly to masked image modeling, that is, we want to find patches with lower reconstruction difficulty within the obtained areas with higher information density.

3. Method

In this section, we first introduce the general idea of AutoMAE in handling the challenges of the patch selection dilemma. We then detail the main components of AutoMAE which can adaptively optimize appropriate masking strategies to facilitate the learning of the masked autoencoder. The framework of AutoMAE is shown in Figure 3.

3.1. General Design of AutoMAE

Motivated by the observations in Section 2.2, we start to design a novel self-supervised framework that can learn to select more informative foreground patches to mask, in which two key challenges need to be properly handled:

- How to guide the ViT model mining the informative foreground patches without any explicit supervision?
- How to control the difficulty of the pretext task via an adaptively learned mask strategy?

For the first challenge, we propose a differentiable mask generator G to generate the mask image which contains the important weight for each image patch. The mask generator contains a pretrained ViT encoder (also in a self-supervised manner) and two trainable convolution layers. Given an input image, we use the pretrained ViT encoder to extract the multi-head attention maps from the last transformer block. The obtained attention maps contain indications of different semantic regions of the image and are further processed by the convolution layers for mask generation. Since we cannot obtain explicit supervision to highlight the location of the foreground object, we introduce an object-centered adversarial training strategy to guide the mask generator in producing higher weights on patches within possible foreground objects. Specifically, we introduce a discriminator and generate real mask images by manually raising the masking probabilities of a randomly sampled rectangle area. In this way, we minimize the distribution distance between the generated mask and the sample real mask, which helps the model find the informative foreground patches.

For the second challenge, we directly propagate the gradients from the masked autoencoder back to the mask generator and train these two modules synchronously. In other

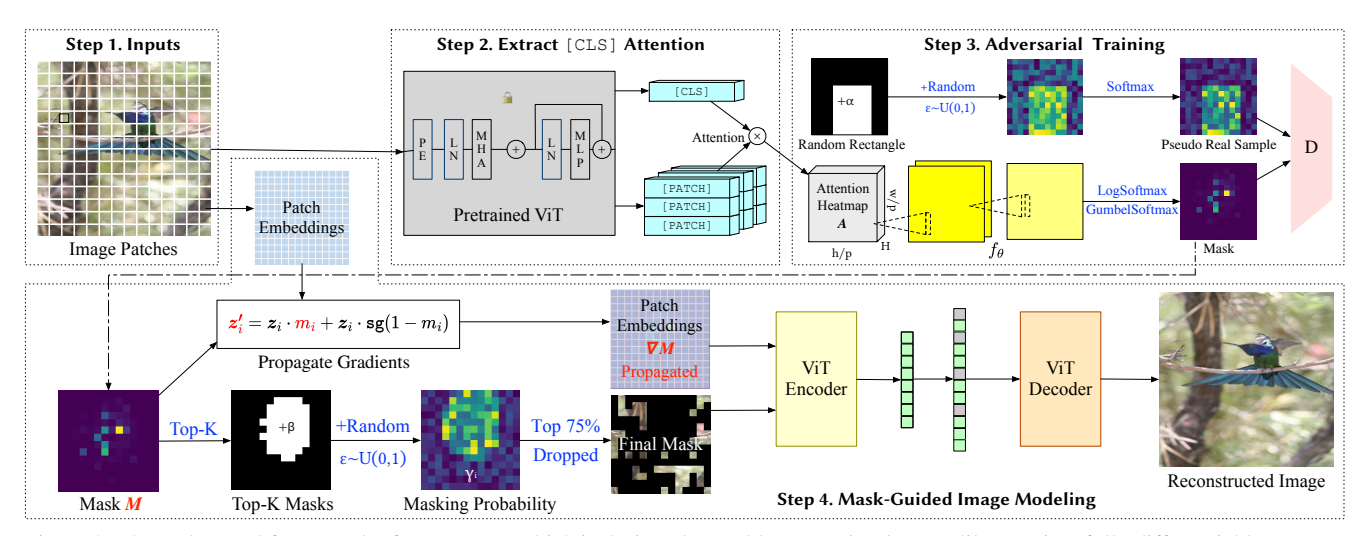


Figure 3. The end-to-end framework of AutoMAE, which is designed to tackle to patch selection dilemma in a fully differentiable manner.

words, the reconstruction loss applied for the masked autoencoder also constrains the mask generator from generating too hard mask images. By this means, the masked autoencoder encourages the mask generator to produce high weights on patches that can easily infer the masking information, while the discriminator regularizes the mask generator and focuses more on possible foreground objects instead of the background. These two branches cooperate with each other to facilitate the masked autoencoder to learn more representative patch relations.

3.2. Adversarially-Trained Mask Generator

The differentiable mask generator G aims to generate sample-specific mask images to guide the token selection process in the training of the masked autoencoder, which mainly consists of a pretrained ViT encoder and two trainable convolutional layers. As shown in Figure 3, we first exploit an MAE-pretrained [3] ViT encoder to embed the image $\mathbf{I} \in \mathbb{R}^{c \times h \times w}$ and extract the multi-head self-attention map $\mathbf{A} \in \mathbb{R}^{H \times \frac{h}{p} \times \frac{w}{p}}$ between the query embedding of the <code>[CLS]</code> token and key embeddings of other patch tokens from the last transformer block, where H represents the number of heads. Specifically, the calculation of the ith attention map $\mathbf{A}_i \in \mathbb{R}^{1 \times \frac{h}{p} \times \frac{w}{p}}$ can be formalized as

$$\boldsymbol{A}_i = \operatorname{softmax}(\boldsymbol{q}_i^c \boldsymbol{K}_i^\top / \sqrt{d'}), \tag{1}$$

where $q_i^c \in \mathbb{R}^{1 \times d'}$ represents the query embedding of the <code>[CLS]</code> token, $\boldsymbol{K}_i \in \mathbb{R}^{\frac{hw}{p^2} \times d'}$ represents the key embeddings of other patch tokens, and d' = d/H represents the embedding dim. Then we reshape the attention map with

spatial size equal to $1 \times \frac{h}{p} \times \frac{w}{p}$. As mentioned in [3], different attention maps in the last transformer block can attend to different semantic regions of the image. Therefore these attention maps can be served as informed initialization for further mask generation. Besides, the parameters of the pretrained ViT encoder are frozen during the training process.

Given the multi-head self-attention map A, we further exploit two convolutional layers with ReLU activation f_{θ} to embed these attention maps:

$$\boldsymbol{F} = f_{\theta}(\boldsymbol{A}), \tag{2}$$

where $m{F} \in \mathbb{R}^{1 \times \frac{h}{p} \times \frac{w}{p}}$. We then sample the final mask image $m{M} \in \mathbb{R}^{1 \times \frac{h}{p} \times \frac{w}{p}}$ given the embedding feature $m{F}$:

$$f'_{i} = \log(\frac{\exp(f_{i})}{\sum_{k=1}^{hw/p} \exp(f_{k})}) + z,$$

$$m_{i} = \frac{\exp(f'_{i})}{\sum_{k=1}^{hw/p} \exp(f'_{k})},$$
(3)

where z represents a random noise sampled from a Gumbel distribution, and the $\log(softmax(\cdot))$ here is used to stable the training process. Now, the values in M are continuous and can be seen as the important weight of each image patch, and we use an extra discriminator and the masked autoencoder itself to supervise the generation process.

Although the attention map \boldsymbol{A} can provide indications for different semantic regions, how to supervise the mask generator to produce a proper pretext task that can focus on foreground objects is still a challenging problem. To tackle this problem, we introduce an extra discriminator and design an object-centered adversarial training strategy to regularize mask generation. The key insight of this approach is to generate pseudo mask images \boldsymbol{M}^p as "real" samples which can imitate the difference between foreground and background patches, and use the adversarial training strat-

¹Various self-supervised pretrained ViT models can be used for attention map extraction, whose effect is compared in the experiments. In the rest of the paper, we adopt the MAE-pretrained ViT-Base model for attention maps extraction without loss of generality.

egy to minimize the distribution shift between generated mask M and "real" samples M^p .

The way to generate pseudo-mask images is quite simple. Given a zero-initialized image $M^p \in \mathbb{R}^{1 \times \frac{h}{p} \times \frac{w}{p}}$, we first randomly sample a rectangle area within this image whose spatial size is between $20\% \sim 80\%$ of the whole image area. This sampled rectangle area is assumed to be the bounding box of one pseudo object. Then we flatten the pseudo mask $M^p = \{m_i^p\}_{i=1}^n$ and suppose the index set within the sample rectangle area is X, the values in the pseudo mask are sampled as follows:

$$m_i^p = \epsilon + \begin{cases} \alpha & i \in \mathbf{X} \\ 0 & i \notin \mathbf{X} \end{cases} \tag{4}$$

where ϵ represents a random noise sampled from a uniform distribution $\epsilon \sim U(0,1)$, and α represents the additional important weight for patches within the rectangle, which is set to 0.5 in our experiments. In this way, we generate the pseudo mask images where foreground patches contain higher weights compared with background patches. We then use the pseudo-mask images as a real sample for adversarial training with the loss function from LSGAN [28]:

$$\mathcal{L}_{\text{adv}} = -\mathbb{E}_{M} \left[(D(\boldsymbol{M}) - c)^{2} \right],$$

$$\mathcal{L}_{\text{adv}}^{D} = \mathbb{E}_{M^{p}} \left[(D(\boldsymbol{M}^{p}) - b)^{2} \right] + \mathbb{E}_{M} \left[(D(\boldsymbol{M}) - a)^{2} \right],$$
(5)

where D represents the discriminator and we set a=-1,b=1,c=0 as used in previous work.

3.3. Mask-Guided Image Modeling

Given the sampled mask M, we suggest that patches with higher weights are more likely to be foreground objects and more informative than patches with lower weights. Therefore, we raise the masking probabilities of these highweighted patches and use low-weighted patches as visible hints in masked image modeling. Specifically, we first sort the values in $M = \{m_1, m_2, \cdots, m_n\}$ and then get the top K index set Y. The unnormalized masking probability of each token can be sampled as follows:

$$\gamma_i = \epsilon + \begin{cases} \beta & i \in \mathbf{Y} \\ 0 & i \notin \mathbf{Y} \end{cases} \tag{6}$$

where ϵ represents a random noise sampled from a uniform distribution $\epsilon \sim U(0,1)$, and β represents the additionally raised probability for tokens with higher weights. In our experiment, we set K=n/4 and $\beta=0.5$ where n represents the number of patch tokens. In this case, patches in set \boldsymbol{Y} are supposed to be more informative than other patches, and models are supposed to pay more attention to these patches.

After that, we use the sampled probability to guide the token selection process where tokens with the top 75%

biggest probability are dropped and the remaining tokens with 25% smallest probability are saved as visible hints for masked image modeling. In other words, we still follow the mask ratio used in the original masked autoencoder while using the sampled probabilities to enhance the learning of more important patches.

Particularly, we slightly change the formulation of the input patch tokens to allow the gradients from the masked autoencoder can be propagated back to the mask generator. Given the embedded patch tokens $\mathbf{Z} = \{\mathbf{z}_i\}_{i=1}^n$ and the generated mask image $\mathbf{M} = \{m_i\}_{i=1}^n$, the new embedded patch tokens $\mathbf{Z'} = \{\mathbf{z'}_i\}_{i=1}^n$ are obtained via

$$\mathbf{z'}_i = \mathbf{z}_i \cdot m_i + \mathbf{z}_i \cdot \operatorname{sg}(1 - m_i), \tag{7}$$

where $sg(\cdot)$ represents the stop gradient operation. We conduct token selection on these new embedded tokens Z' and then perform the following encoding and decoding stages which are the same as the original masked autoencoder. In this way, we preserve the values of patch tokens while allowing the masked autoencoder can also influence the mask generation. Combined with the adversarial loss, the full objective function of the mask generator can be written as

$$\mathcal{L}_{G} = \mathcal{L}_{recon} + \lambda \mathcal{L}_{adv}, \tag{8}$$

where we set $\lambda = 0.2$ by grid search.

4. Experiments

We evaluate AutoMAE in the linear probing and finetuning setups on ImageNet-1K [10], and perform model analyses on its smaller subsets. We also conduct transfer learning experiments on CUB-Bird [37], Stanford-Cars [22], iNaturalist 2019 [36], COCO [26], and ADE20K [47] for finegrained classification, detection, and segmentation tasks.

We use the same ViT-Base architecture and a 16×16 patch size in all compared models. For AutoMAE, we typically use an 800-epochs-pretrained MAE-Base (called "MAE-800") as the warmup model of the feature extractor in mask generation. We freeze its parameters and train other parts of AutoMAE for 800 epochs. We use SemMAE [23] as our primary baseline as its mask generator also uses a warmup model². Since its training code was not publicly available until the last week before the paper submission deadline, we can only use the provided SemMAE pretrained model with a 16×16 patch size.

We further discuss the architecture of the mask discriminator, the way of hyperparameter tuning, other training details, and time cost in the supplementary materials.

4.1. Model Analyses

We conduct model analyses in the linear probing setup by pretraining the models on smaller subsets of ImageNet-1K. Specifically, we randomly sample $10\% \sim 30\%$ images

²SemMAE [23] uses an 800-epochs iBOT model in the mask generator.

Model	Warmup in G	Acc-1(%)
MAE [16]	N/A	50.50
— w/ bounding box	N/A	52.52
AutoMAE	MAE-400-Small	53.57
AutoMAE	MAE-800	53.58
— Two-Stage	MAE-800	52.57
-G: MAE-Max	MAE-800	50.85
AutoMAE	DINO-B	53.20
G: DINO-Max	DINO-B	51.52

Table 1. Linear probing accuracy of models pretrained on a 30% subset of ImageNet-1K for 400 epochs. All models are on the full validation set of ImageNet-1K. We use different ViT backbones with frozen parameters in the mask generator.

Model	Warmup in G	Acc-1(%)
MAE [16]	N/A	23.07
AutoMAE	MAE-800	26.84
AutoMAE	From-Scratch	26.00
— w/ EMA $m = 0.9$	From-Scratch	25.92
— w/ EMA $m = 0.99$	From-Scratch	25.45

Table 2. Linear probing of models pretrained on 10% ImageNet for 400 epochs. AutoMAE significantly outperforms the original MAE pertaining even with a randomly initialized mask generator.

and perform the pretraining for 400 epochs. For linear probing, we finetune the model for 90 epochs and evaluate it on the **full** ImageNet-1K validation set.

Mask generator with a pretrained ViT. In Table 1, we compare the use of different self-supervised warmup methods (MAE-800 vs. MAE-400-Small) for the ViT-Base feature extractor in the mask generator. The latter one is *pretrained on the* 30% *subset for* 400 *epochs*. It achieves a comparable Top-1 accuracy (53.57%) with the one with the MAE-800 backbone (53.58%), which is significantly higher (+2.89) than its baseline MAE (50.50%) and the best MAE model with ground-truth bounding box guidance (as described in Section 2.2). These results indicate that the main improvement in the performance of AutoMAE comes from the differentiable mask sampling method, as the mask generator is effective even with a weak feature extractor.

Mask generator without a pretrained ViT. In most of the experiments, the mask generator of AutoMAE relies on a pretrained ViT. We here consider removing such a requirement by using a train-from-scratch ViT backbone. The simplest way is to **reuse** the same ViT model for both mask generation and mask reconstruction. As shown in Table 2, this model ("From-Scratch") remarkably outperforms the vanilla MAE model (26.00% vs 23.07%), both pretrained on the 10% ImageNet subset. It suggests that AutoMAE is effective even without any pretrained models. We further perform the exponential moving average

β	0.2	0.5	1.0
Linear probing	52.04	53.58	53.43

Table 3. Linear probing accuracy with different margin values.

Original	Top 10%	Top 25%	Top 50%	Top 75%

Figure 4. High-weighted masks on **ImageNet-9** produced by the mask generator. The highlighted areas are obtained from the mask before adding random noise by K-largest values, not final masks.

(EMA) to synchronize the ViT used for mask generation (k) and the one used for image reconstruction (q). We have $\theta_k = m \times \theta_k + (1-m) \times \theta_q$. Results are shown in Table 2.

On joint training. We conduct an ablation study of AutoMAE by separating it into two independent learning processes, *i.e.*, mask generation and mask-guided image modeling. In Table 1, the "Two-stage" model outperforms MAE (52.57% vs 50.50%) but underperforms the joint training version (53.58%), which validates the effectiveness of joint training in AutoMAE. In Table 4 (*full-set pretraining*), we compare AutoMAE with SemMAE, a two-stage pretraining pipeline with an independent mask learning stage. It further supports the superiority of joint training over two-stage training (66.7% vs. 65.0%).

On adversarial mask generation. As DINO [3] suggests that the last self-attention layer in ViT blocks can provide meaningful masks, we remove the adversarial training loss and replace the two-layer CNN in the mask generator (after the feature extractor) with a simple maximum operator over the channel axis. From Table 1, although these models ("MAE-Max & DINO-Max") still outperform the original MAE, they obtain lower accuracy than corresponding AutoMAE models with MAE-800 and DINO-B. It indicates that the mask generator does learn a better masking function than simply taking the maximum attention values.

Sensitivity analysis on the margin value β . Previously in Figure 2, we show how the margin value of the masking probability β affects the linear probing performance with bounding box guidance. Here, as shown in Table 3, we conduct a grid search over $\beta = \{0.2, 0.5, 1.0\}$ on the ImageNet subset and find that $\beta = 0.5$ performs best.

Mask visualization. To verify whether the mask generator can perceive meaningful areas, we conduct experiments on ImageNet-9 [40], a dataset with foreground objects only.

Model	Warmup in G	Acc-1(%)
MAE [16]	N/A	63.7
SemMAE [23]	iBOT-800	65.0
AutoMAE	MAE-800	<u>66.7</u>
AutoMAE	iBOT-B [48]	<u>66.7</u>
AutoMAE	DINO-S [3]	68.8

Table 4. Linear probing results of models pretrained on the full ImageNet for 800 epochs. Regardless of the methods used in the mask generator to warm up its feature extractor, AutoMAE consistently achieves better performance.

Model	Warmup in G	Ratio	Acc-1(%)
MAE [16]	N/A	100	83.26
SemMAE [23]	iBOT-800	100	83.34
AutoMAE	MAE-800	100	83.32
MAE [16]	N/A	30	78.95
SemMAE [23]	MAE-800	30	79.00
AutoMAE	MAE-800	30	79.14

Table 5. Finetuning results on ImageNet-1K. "Ratio" represents the percentage of the data we used for finetuning. All methods use ViT-Base as the encoder with a patch size of 16×16 .

As shown in Figure 4, the most high-weighted masks in AutoMAE mainly focus on meaningful patches, such as the back and eyes of the jaguar, and gradually involve less significant patches as the masking ratio increases. More results are provided in supplementary materials.

4.2. Experiments on ImageNet-1K

When we have finished the preliminary model analyses on small subsets, we start to train AutoMAE on the full ImageNet-1K and analyze the experimental results.

Linear probing. We use 3 alternative models to initialize the feature extractor in the mask generator: (1) the ViT-B network pretrained with MAE [16] (termed as MAE-800), (2) the ViT-B pretrained with iBOT [48] (termed as iBOT-B), and (3) the ViT-S pretrained with DINO [3] (termed as DINO-S). We use the LARS optimizer to train the model for 90 epochs. The base learning rate is set to 0.1, the momentum is 0.9, and the batch size is 16,384. We use random resized cropping and horizontal flipping for data augmentation. As shown in Table 4, AutoMAE consistently achieves better performance than the vanilla MAE model, regardless of the base models used for mask generation.

Finetuning. In the finetuning stage, the base learning rate is set to 5×10^{-4} and the AdamW momentum is configured as $\beta_1, \beta_2 = 0.9, 0.999$. The effective batch size is 1,024. Similar to previous literature, we use the RandAug technique [8] for data augmentation and employ layer-wise learning rate decay (0.75), Mixup [46] (0.8), CutMix [44] (1.0), and DropPath [19] (0.1) in the finetuning stage. All

Method	Ratio(%)	CUB	Cars	iNat-19
MAE [16]	100	83.3	92.7	79.50
SemMAE [23]	100	82.1	92.4	79.60
AutoMAE	100	83.7	93.1	79.93
MAE [16]	50	70.6	84.2	73.76
SemMAE [23]	50	70.6	82.1	73.47
AutoMAE	50	73.4	84.6	74.03
MAE [16]	10	-	-	49.14
SemMAE [23]	10	-	-	48.65
AutoMAE	10	-	-	50.13

Table 6. Fine-grained classification results. All methods exploit ViT-Base as the encoder with a patch size equal to 16×16 . "Ratio" is the percentage of data used in fine-tuning. Ratio 10% for CUB and Cars is omitted because the two datasets are not large enough.

Method	Pretrain Epochs	APbox	APmask
BEiT* [1]	800	49.8	44.4
MAE* [16]	1600	50.3	44.9
AutoMAE	800	50.5	45.0

Table 7. Results of object detection and instance segmentation on the COCO dataset. * indicates results from the original literature.

compared models are trained for 100 epochs in the same setting. As shown in Table 5, our approach achieves competitive results to MAE and SemMAE. It is reasonable that SemMAE has a slightly better performance on full-set fine-tuning, as it uses an iBOT-based mask generator which is pretrained by contrastive learning. It is also worth noting that SemMAE with a 16×16 patch size obtains similar fine-tuning results, indicating that the non-linear features for big tokens in MAE are strong enough for image classification. Furthermore, we perform an additional experiment to fine-tune the models on the 30% subset. As shown in Table 5, AutoMAE outperforms MAE and SemMAE by large margins, suggesting that it is more effective in scenarios with limited data.

4.3. Downstream Tasks

We here provide the transfer learning results on a wide range of downstream tasks. All of the compared models are pretrained on the full ImageNet-1K dataset.

Fine-grained image classification. We first finetune the models on fine-grained image classification datasets, including CUB-Bird [37], Stanford-Cars [22], and iNaturalist 2019 [36]. As shown in Table 6, AutoMAE achieves the best performance on all datasets. Similarly, we experiment with random-sampled subsets (50% and 10%), where AutoMAE shows more significant improvements compared with other models. These results demonstrate the promising transfer learning ability of our method to small datasets.

Model	Ratio(%)	mIoU
Supervised Pretraining	100	45.3
BEiT* [1]	100	45.8
MAE [16]	100	46.1
SemMAE [23]	100	46.3
AutoMAE	100	46.4
MAE [16]	50	41.7
SemMAE [23]	50	41.9
AutoMAE	50	42.4

Table 8. Results of semantic segmentation on ADE20K. "Ratio" is the percentage of data used in finetuning.

Object detection and instance segmentation. Table 7 gives the detection and instance segmentation results on COCO. We follow the previous work [24] to finetune the Mask-RCNN [18] with a ViT-based FPN backbone. Due to the memory limit, we set the total batch size to 32, half of the original value, and set the learning rate to 4×10^{-5} . We finetune AutoMAE for 100 epochs which is the same as the compared models. It shows that even though AutoMAE is pretrained for half epochs (800), it still outperforms the original MAE by 0.2 in AP^{box} and 0.1 in AP^{mask}.

Semantic segmentation. We use the ADE20K dataset for semantic segmentation, which contains 150 semantic categories and 25K images. Similar to SemMAE [47], we use UperNet [41] as the network backbone to finetune the pretrained ViT-B network for 160K iterations on ADE20K. The learning rate is set to 5×10^{-5} and the batch size is 8. We also finetune our pretrained model for 100 epochs which is the same as other compared methods. As shown in Table 8, AutoMAE outperforms MAE by 0.3 mIoU and outperforms SemMAE by 0.1 mIoU. We then use fewer data (50%) in the finetuning stage. Similar to our previous findings, we observe that AutoMAE achieves a more significant advantage over MAE and SemMAE in this case, increasing mIoU results by 0.7 and 0.5, respectively.

5. Related Work

The majority of recent studies of self-supervised learning for visual representations of deep networks can be roughly grouped into two categories, *i.e.*, contrastive learning and masked image modeling.

Contrastive learning methods typically distinguish positive samples from other samples. Starting with InfoNCE [35], finding an efficient way of generating high-quality samples is a critical concern in this field. Memory bank [39] stores all samples to enlarge the sample space. MoCo [17, 6] designs a queue-based memory bank with momentum update to break the limit of batch size. SimCLR [5] introduces strong augmentations and MLP projection heads without a memory bank. BYOL [15] introduces a predic-

tor module with gradient stopping to remove the need for negative pairs. SimSiam [7] further simplifies BYOL by removing the momentum encoder. DINO [3] also eliminates the requirement of negative pairs by self-distillation. UniGrad [31] unifies common contrastive learning methods [17, 5, 7, 32, 15, 45, 2] into the same form.

Recent studies in masked image modeling (MIM) [13, 34, 12, 1, 4] are largely inspired by the success of BERT [11]. According to different regression targets, MIM methods can be divided into two groups: pixel-level reconstruction and feature-level prediction. Feature-level prediction usually requires an external model called "Tokenizer" to generate reconstruction targets. BEiT [1] and PeCo [29] are pretrained to predict visual tokens generated by discrete variational autoencoder (dVAE) following DALL-E [29]. iBOT [48] presents an online tokenizer as the teacher network to produce the target and perform self-distillation. MaskFeat [38] proposes HOG [9] to pretrain video models without tokenization. On the other hand, pixel-level reconstruction methods directly use raw pixel values as the regression targets. MAE [16] and SimMIM [42] show that masking a high ratio of patches and directly predicting RGB values can achieve BEiT-level performance. MC-MAE [14] demonstrates a hybrid convolution-transformer with a multi-scale feature design can boost the performance of MAE. CMAE [20] combines contrastive learning and MIM with augmentations and feature alignment.

The group of work most relevant to AutoMAE includes methods that also improve masking strategies in MIM. SemMAE [23] adopts a two-stage framework that first learns a part indicator and then fixes it in the MIM training stage. AttMask [21] presents an independently-trained self-attention module to mask high-attended patches, while MST [25] proposes to mask low-attended patches. the above discussions, we empirically show the superiority of the proposed differentiable framework over two-stage training. ADIOS [30] combines an adversarial MIM with contrastive learning. In contrast, AutoMAE does not rely on contrastive learning but rather introduces prior hints through adversarial training. Furthermore, AutoMAE does not require expensive multiple forward passes in a single training iteration. The experiments of ADIOS are mainly conducted on small datasets such as STL10 and a downsized version of ImageNet-100 [33], which supports the validity of our model analysis setup on the ImageNet subsets.

6. Conclusion

In this paper, we focused on improving the masking strategy that was shown to play an important role in the masked image modeling framework. We illustrated that introducing object-centric priors to guide the masking strategy can significantly improve the learned visual representations. Starting from this point, we proposed AutoMAE,

which integrates a differentiable mask generator to provide the sample-specific categorical distribution of masking probabilities across all image patches. The mask generator is jointly trained with the ViT model with an adversarial learning constraint. We validated the effectiveness of AutoMAE on different benchmarks and downstream tasks.

References

- [1] Hangbo Bao, Li Dong, Songhao Piao, and Furu Wei. Beit: BERT pre-training of image transformers. In *ICLR*, 2022. 7,
- [2] Adrien Bardes, Jean Ponce, and Yann LeCun. Vicreg: Variance-invariance-covariance regularization for selfsupervised learning. In *ICLR*, 2022. 8
- [3] Mathilde Caron, Hugo Touvron, Ishan Misra, Hervé Jégou, Julien Mairal, Piotr Bojanowski, and Armand Joulin. Emerging properties in self-supervised vision transformers. In *ICCV*, 2021. 4, 6, 7, 8
- [4] Mark Chen, Alec Radford, Rewon Child, Jeffrey Wu, Heewoo Jun, David Luan, and Ilya Sutskever. Generative pretraining from pixels. In *ICML*, 2020. 8
- [5] Ting Chen, Simon Kornblith, Mohammad Norouzi, and Geoffrey Hinton. A simple framework for contrastive learning of visual representations. In *ICML*, 2020. 8
- [6] Xinlei Chen, Haoqi Fan, Ross B. Girshick, and Kaiming He. Improved baselines with momentum contrastive learning. CoRR, 2020. 8
- [7] Xinlei Chen and Kaiming He. Exploring simple siamese representation learning. In CVPR, 2021.
- [8] Ekin D Cubuk, Barret Zoph, Jonathon Shlens, and Quoc V Le. Randaugment: Practical automated data augmentation with a reduced search space. In CVPR workshops, 2020. 7
- [9] Navneet Dalal and Bill Triggs. Histograms of oriented gradients for human detection. In CVPR, 2005.
- [10] Jia Deng, Wei Dong, Richard Socher, Li-Jia Li, Kai Li, and Li Fei-Fei. Imagenet: A large-scale hierarchical image database. In CVPR, 2009. 2, 3, 5
- [11] Jacob Devlin, Ming-Wei Chang, Kenton Lee, and Kristina Toutanova. BERT: pre-training of deep bidirectional transformers for language understanding. In NAACL-HLT, 2019.
- [12] Alexey Dosovitskiy, Lucas Beyer, Alexander Kolesnikov, Dirk Weissenborn, Xiaohua Zhai, Thomas Unterthiner, Mostafa Dehghani, Matthias Minderer, Georg Heigold, Sylvain Gelly, Jakob Uszkoreit, and Neil Houlsby. An image is worth 16x16 words: Transformers for image recognition at scale. In *ICLR*, 2021. 1, 8
- [13] Christoph Feichtenhofer, Haoqi Fan, Yanghao Li, and Kaiming He. Masked autoencoders as spatiotemporal learners. In *NeurIPS*, 2022. 8
- [14] Peng Gao, Teli Ma, Hongsheng Li, Ziyi Lin, Jifeng Dai, and Yu Qiao. Mcmae: Masked convolution meets masked autoencoders. In *NeurIPS*, 2022. 8
- [15] Jean-Bastien Grill, Florian Strub, Florent Altché, Corentin Tallec, Pierre Richemond, Elena Buchatskaya, Carl Doersch,

- Bernardo Avila Pires, Zhaohan Guo, Mohammad Gheshlaghi Azar, et al. Bootstrap your own latent-a new approach to self-supervised learning. In *NeurIPS*, 2020. 8
- [16] Kaiming He, Xinlei Chen, Saining Xie, Yanghao Li, Piotr Dollár, and Ross Girshick. Masked autoencoders are scalable vision learners. In CVPR, 2022. 1, 2, 6, 7, 8, 11
- [17] Kaiming He, Haoqi Fan, Yuxin Wu, Saining Xie, and Ross Girshick. Momentum contrast for unsupervised visual representation learning. In CVPR, 2020. 8
- [18] Kaiming He, Georgia Gkioxari, Piotr Dollár, and Ross B. Girshick. Mask R-CNN. In ICCV, 2017. 8
- [19] Gao Huang, Yu Sun, Zhuang Liu, Daniel Sedra, and Kilian Q. Weinberger. Deep networks with stochastic depth. In ECCV, 2016. 7
- [20] Zhicheng Huang, Xiaojie Jin, Chengze Lu, Qibin Hou, Ming-Ming Cheng, Dongmei Fu, Xiaohui Shen, and Jiashi Feng. Contrastive masked autoencoders are stronger vision learners. CoRR, 2022. 8
- [21] Ioannis Kakogeorgiou, Spyros Gidaris, Bill Psomas, Yannis Avrithis, Andrei Bursuc, Konstantinos Karantzalos, and Nikos Komodakis. What to hide from your students: Attention-guided masked image modeling. In ECCV, 2022.
- [22] Jonathan Krause, Michael Stark, Jia Deng, and Li Fei-Fei. 3d object representations for fine-grained categorization. In *ICCV Workshops*, 2013. 2, 5, 7
- [23] Gang Li, Heliang Zheng, Daqing Liu, Chaoyue Wang, Bing Su, and Changwen Zheng. Semmae: Semantic-guided masking for learning masked autoencoders. In *NeurIPS*, 2022. 1, 2, 3, 5, 7, 8
- [24] Yanghao Li, Saining Xie, Xinlei Chen, Piotr Dollár, Kaiming He, and Ross B. Girshick. Benchmarking detection transfer learning with vision transformers. *CoRR*, 2021. 8
- [25] Zhaowen Li, Zhiyang Chen, Fan Yang, Wei Li, Yousong Zhu, Chaoyang Zhao, Rui Deng, Liwei Wu, Rui Zhao, Ming Tang, et al. Mst: Masked self-supervised transformer for visual representation. In *NeurIPS*, 2021. 8
- [26] Tsung-Yi Lin, Michael Maire, Serge J. Belongie, James Hays, Pietro Perona, Deva Ramanan, Piotr Dollár, and C. Lawrence Zitnick. Microsoft COCO: common objects in context. In ECCV, 2014. 2, 5
- [27] Ilya Loshchilov and Frank Hutter. Decoupled weight decay regularization. In 7th International Conference on Learning Representations, ICLR 2019, New Orleans, LA, USA, May 6-9, 2019, 2019.
- [28] Xudong Mao, Qing Li, Haoran Xie, Raymond Y. K. Lau, Zhen Wang, and Stephen Paul Smolley. Least squares generative adversarial networks. In *ICCV*, 2017. 5, 11
- [29] Aditya Ramesh, Mikhail Pavlov, Gabriel Goh, Scott Gray, Chelsea Voss, Alec Radford, Mark Chen, and Ilya Sutskever. Zero-shot text-to-image generation. In *ICML*, 2021. 8
- [30] Yuge Shi, N Siddharth, Philip Torr, and Adam R Kosiorek. Adversarial masking for self-supervised learning. In *ICML*, 2022. 8
- [31] Chenxin Tao, Honghui Wang, Xizhou Zhu, Jiahua Dong, Shiji Song, Gao Huang, and Jifeng Dai. Exploring the equivalence of siamese self-supervised learning via a unified gradient framework. In *CVPR*, 2022. 8

- [32] Yuandong Tian, Xinlei Chen, and Surya Ganguli. Understanding self-supervised learning dynamics without contrastive pairs. In *ICML*, 2021. 8
- [33] Yonglong Tian, Dilip Krishnan, and Phillip Isola. Contrastive multiview coding. In ECCV, 2020. 8
- [34] Zhan Tong, Yibing Song, Jue Wang, and Limin Wang. Videomae: Masked autoencoders are data-efficient learners for self-supervised video pre-training. In *NeurIPS*, 2022. 8
- [35] Aäron van den Oord, Yazhe Li, and Oriol Vinyals. Representation learning with contrastive predictive coding. *CoRR*, 2018. 8
- [36] Grant Van Horn, Oisin Mac Aodha, Yang Song, Yin Cui, Chen Sun, Alex Shepard, Hartwig Adam, Pietro Perona, and Serge Belongie. The inaturalist species classification and detection dataset. In CVPR, 2018. 2, 5, 7
- [37] Catherine Wah, Steve Branson, Peter Welinder, Pietro Perona, and Serge J. Belongie. The caltech-ucsd birds-200-2011 dataset. 2011. 2, 5, 7
- [38] Chen Wei, Haoqi Fan, Saining Xie, Chao-Yuan Wu, Alan Yuille, and Christoph Feichtenhofer. Masked feature prediction for self-supervised visual pre-training. In CVPR, 2022.
- [39] Zhirong Wu, Yuanjun Xiong, Stella X Yu, and Dahua Lin. Unsupervised feature learning via non-parametric instance discrimination. In CVPR, 2018. 8
- [40] Kai Xiao, Logan Engstrom, Andrew Ilyas, and Aleksander Madry. Noise or signal: The role of image backgrounds in object recognition. In *ICLR*, 2021. 6
- [41] Tete Xiao, Yingcheng Liu, Bolei Zhou, Yuning Jiang, and Jian Sun. Unified perceptual parsing for scene understanding. In ECCV, 2018. 8
- [42] Zhenda Xie, Zheng Zhang, Yue Cao, Yutong Lin, Jianmin Bao, Zhuliang Yao, Qi Dai, and Han Hu. Simmim: A simple framework for masked image modeling. In CVPR, 2022. 1, 8
- [43] Yuichi Yoshida and Takeru Miyato. Spectral norm regularization for improving the generalizability of deep learning. *CoRR*, 2017. 11
- [44] Sangdoo Yun, Dongyoon Han, Sanghyuk Chun, Seong Joon Oh, Youngjoon Yoo, and Junsuk Choe. Cutmix: Regularization strategy to train strong classifiers with localizable features. In *ICCV*, 2019. 7
- [45] Jure Zbontar, Li Jing, Ishan Misra, Yann LeCun, and Stéphane Deny. Barlow twins: Self-supervised learning via redundancy reduction. In *ICML*, 2021. 8
- [46] Hongyi Zhang, Moustapha Cissé, Yann N. Dauphin, and David Lopez-Paz. mixup: Beyond empirical risk minimization. In *ICLR*, 2018. 7
- [47] Bolei Zhou, Hang Zhao, Xavier Puig, Tete Xiao, Sanja Fidler, Adela Barriuso, and Antonio Torralba. Semantic understanding of scenes through the ade20k dataset. In *ICCV*, 2019. 2, 5, 8
- [48] Jinghao Zhou, Chen Wei, Huiyu Wang, Wei Shen, Cihang Xie, Alan Yuille, and Tao Kong. ibot: Image bert pre-training with online tokenizer. In *ICLR*, 2022. 7, 8

Appendices

A. Implementation Details

Model architecture. In adversarial training, we use a three-layer CNN as the discriminator as shown in Figure A1. For all experiments, we use the ViT-Base with a patch size equal to 16×16 as the encoder architecture in MAE. For the mask generator, we exploit an MAE-pretrained ViT-Base encoder to extract the attention maps from the input image. This ViT-Base encoder is pretrained on the ImageNet dataset for 800 epochs and frozen during the training of the mask generator, termed as "MAE-800". we also try other pretrained models as the mask generator and provide results in the following sections.

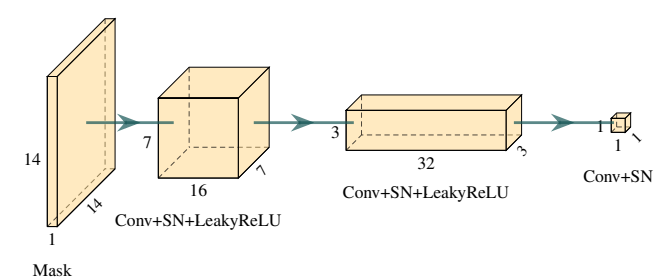


Figure A1. The architecture of the mask discriminator. SN denotes Spectral Normalization [43] and LeakyReLU has a slope of -0.2. As a common practice, input images of AutoMAE are resized to 224×224 . We use a 16×16 patch size and the mask feature map generated by the two-layer mask generator has a size of 14×14 .

Training details. We adopt the AdamW optimizer [27] for pretraining the MAE model and the mask generator in our AutoMAE. Following previous work [16], the base learning rate is set to 1.5×10^{-4} , the momentum is configured as $\beta_1 = 0.9, \beta_2 = 0.95$, and the batch size is 4,096. We use the linear learning rate schedule: $lr = base_lr \times lr$ batchsize /256. The weight decay is 0.05. The learning rate is scheduled by cosine decay with a warm-up phase of 40 epochs and the total number of pretraining epochs is set to 800. We use random resized cropping and random horizontal flipping for data augmentation. For the discriminator, we use the Adam optimizer without the weight decay. Other hyper-parameters stay the same. The mask generator uses a margin of $\alpha = 0.5$ to highlight the randomly sampled foreground area, and the loss weight λ is set to 0.2 to balance generator loss with reconstruction loss.

Hyperparameters. In Eq.(4) and Eq.(6), we set $\alpha = \beta$ as they have similar effects. In Eq.(5), the values of a,b,c are directly taken from LSGAN [28]. We only tune β and the loss weight λ on the ImageNet subset (30%), and reuse the obtained values in other datasets/setups.

Training cost We use a patch size of 16×16 for all experiments. It takes about 26 hours to pretrain AutoMAE

models on 30% of ImageNet with 8 NVIDIA RTX 3080Ti graphic cards for 400 epochs, and about 7 days to pretrain AutoMAE models on the full ImageNet dataset with 8 NVIDIA A100 graphic cards for 800 epochs. Admittedly, MAEs commonly benefit from a smaller 8×8 patch size. However, we cannot afford its training cost, *e.g.*, it takes about 4 weeks for 800 epochs on the full ImageNet-1K. We want this paper to focus more on the proposed training scheme than on hyper-parameter tuning. Therefore, we follow the standard 16×16 setup [16, 46], which does not affect the main conclusions when compared to SemMAE.

As shown in Table A1, AutoMAE has comparable time cost to recent advances in self-supervised pre-training [21, 23] based on the same hardware (8×A100 GPUs). The full model has a similar number of parameters and FLOPs to existing work.

B. Visualization

After passing the ViT attention feature map to the two-layer CNN generator, the mask is obtained by applying $\log(\operatorname{softmax}(\cdot))$ and Gumbel softmax. Due to the randomness of Gumbel, we take the output of $\log(\operatorname{softmax}(\cdot))$ and highlight those tokens with the top 25% probability. These tokens are visualized in Figures A2-A4 as white patches.

Figures A2-A4 indicate that the mask generator can learn the information of foreground objects. We can see that at the beginning of training, the mask has no specific patterns. After a certain period of training, it becomes focused on the foreground object. It can even follow the shape of discrete parts (see showcases 15 and 16). It shows that the mask tends to fit the shape of the foreground object best at the early stage (see showcases 3, 5-11). For complex scenes in Figure A4, it still generates meaningful masks around at least one foreground object. Although the generated mask is gradually changed during the pretraining process, it is mainly focused on the area around the foreground, which indicates that it will have a high probability to be dropped in AutoMAE. It proves that our model can generate semantic masks to improve the self-supervised learning process of the original MAE.

Method	Time (@800 epochs)	# Params in total	FLOPs	Hyper-parameters to tune	Better results
SemMAE [23]	6 days	Unknown	Unknown	Partitions, Blur kernel, γ , Patch size, λ	1/7 setups
AttMask [21]	> 8 days	188.10M	37.03G	#Attn layers, p , r , s , λ (see [21] for details)	_
AutoMAE (ours)	7 days	198.08M	35.72G	$\alpha = \beta, \lambda$	6/7 setups

Table A1. Further comparisons. The mask generators in SemMAE and AutoMAE are both based on the pre-trained ViT encoder, while AutoMAE performs better in 6/7 setups: Linear probing, 30% fine-tuning, 100%&50% fine-grained cls, detection, and segmentation.



Figure A2. Masked patches by AutoMAE during the pretraining for 800 epochs. White patches are the output of $\log(\operatorname{softmax}(\cdot))$ with the top 25% probability.



Figure A3. Masked patches by AutoMAE during the pretraining for 800 epochs. White patches are the output of $\log(\operatorname{softmax}(\cdot))$ with the top 25% probability.

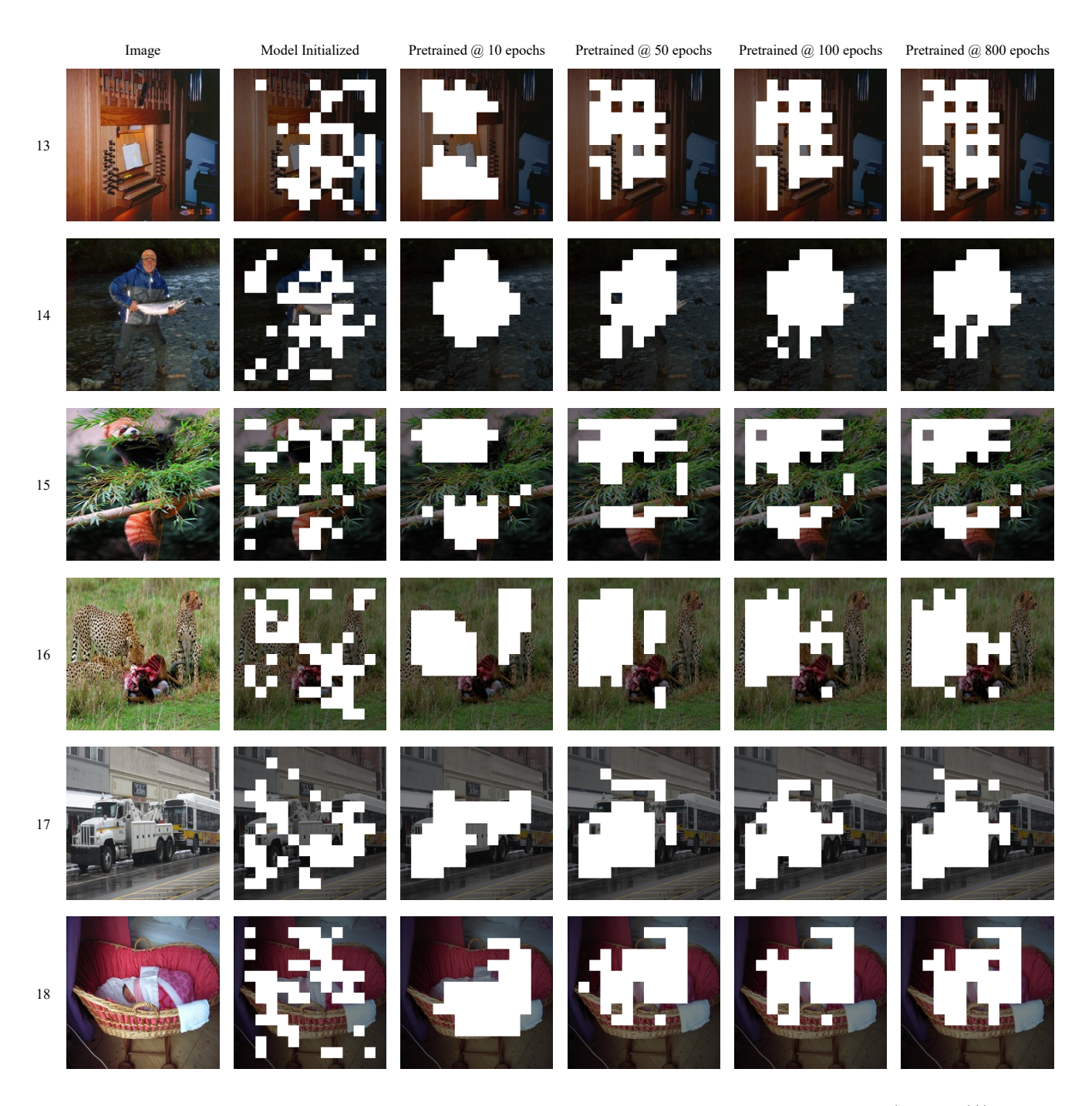


Figure A4. Masked patches by AutoMAE during the pretraining for 800 epochs. White patches are the output of $\log(\operatorname{softmax}(\cdot))$ with the top 25% probability.